Graphitic Nanofilms as Precursors to Wurtzite Films: Theory

Colin L. Freeman, Frederik Claeyssens, and Neil L. Allan
School of Chemistry, University of Bristol, Cantock's Close, Bristol BS8 1TS, United Kingdom

John H. Harding
Department of Engineering Materials, University of Sheffield, Sir Robert Hadfield Building, Mappin Street, Sheffield S1 3JD, United Kingdom

(Received 2 November 2005; published 13 February 2006)

Periodic *ab initio* density functional calculations on ultrathin films of AlN, BeO, GaN, SiC, ZnO, and ZnS demonstrate the stabilization of thicker films terminating with the polar {0001} surface via charge transfer and metallization of the surface layers. In contrast thinner films remove the dipole by adopting a graphiticlike structure in which the atoms are threefold coordinate. This structure is thermodynamically the most favorable for these thinner films. Implications for the crystal growth of wurtzite materials are discussed.

DOI: 10.1103/PhysRevLett.96.066102 PACS numbers: 68.35.Bs, 73.20.At, 81.10.Aj, 81.15.Aa

The wurtzite structure is adopted by a wide range of materials, including semiconductors such as AlN, GaN, and ZnO, which demonstrate many interesting nanostructures such as belts, helices [1], and tubes [2]. For ZnO, the tubes have demonstrated ultraviolet lasing at room temperatures [3]. Their wide, tunable, band gap means these materials find a variety of uses in the electronics industry, e.g., UV light-emitting diodes, laser diodes, solar cells, microsensors, and photocatalysts. Many techniques have been employed to grow wurtzite films including chemical vapor deposition, spray pyrolysis, and pulsed laser deposition and, surprisingly, most of these methods produce c-axis orientated material with a polar morphology. This is a Tasker type III [4] polar surface with either the cation (0001) or anion $(000\bar{1})$ outermost, leading to a divergence of the surface energy that makes the surface intrinsically unstable. Several possible mechanisms for stabilizing the polar surfaces have been suggested (see, e.g., [5] for a review) including adsorption of H adatoms [6], vacancy formation [7], and massive surface reconstructions [8]. A further possibility is a change in the surface electronic structure as suggested for ZnO by Wander *et al.* [9] and Carlsson [10], involving charge transfer from the anion to the cation surface to remove the dipole.

In this Letter we examine the polar nanofilms of a range of wurtzite materials and demonstrate a novel mechanism involving a transition to a graphiticlike structure to remove the dipole. In addition, we propose that charge transfer is a *general* stabilization process for wurtzite films.

We chose to model the polar $(0001)/(000\bar{1})$ and, for comparison, nonpolar $(10\bar{1}0)$ surfaces of AlN, BeO, GaN, SiC, ZnS, and ZnO. The films were modeled as an infinite set of slabs by periodically repeating an appropriately orientated supercell in three dimensions. To ensure a negligible interaction between the slabs, they were each separated by a vacuum gap of $\sim$14 Å. The number of layers present in each film was increased from four until the cleavage energy of the film had converged with respect to the number of layers for both the polar and nonpolar surfaces. Our calculations used periodic plane wave density functional theory (DFT) with the generalized gradient approximation as implemented in the CASTEP 4.2 code [11] with the Perdew-Wang exchange-correlation functional [12]. We used ultrasoft Vanderbilt pseudopotentials [13] and an energy cutoff of 380 eV. The reciprocal space integration scheme utilized the Monkhorst-Pack sampling scheme [14] and we have checked the convergence of the energy with the number of k points. Our geometry optimizations relaxed all degrees of freedom.

Examining the electronic structure of the films demonstrates a clear difference between the polar and nonpolar films. *All* the relaxed {0001} films beyond a certain thickness (see later) show the metallized surface solution described by Wander *et al.* [9] and Carlsson [10] for ZnO (see also [15]). In contrast, the nonpolar $(10\bar{1}0)$ films are insulating. For example, Fig. 1 shows the band structures of bulk wurtzite and a {0001} film of GaN. Metallization of the {0001} film has clearly taken place.

The results of Mulliken charge analyses of these $(0001)/(000\bar{1})$ solutions are presented in Table I. The size of the charge transfer to the cation surface varies between the different films from $\sim 0.27e$ (SiC) to $\sim 0.03e$ (ZnS). We find that the charge transfer is highly restricted to the surface layers and the charge on the atoms in the other layers is generally close to that in the bulk wurtzite. The charge on the anions in the $(000\bar{1})$ surface is very similar to that of the anions in the layer adjacent to the (0001) surface [the (0001) surface bilayer]. For example, in BeO, the charge on the O in the slab interior is $-0.8e$ while the charges on the O are $-0.77e$ and $-0.83e$ in the $(000\bar{1})$ and (0001) surface bilayers, respectively, a variation of only $0.06e$. In contrast, the charge on the cations varies far more between the slab interior and the surface bilayers. In BeO, the Be in the slab interior has a charge of $+0.8e$,

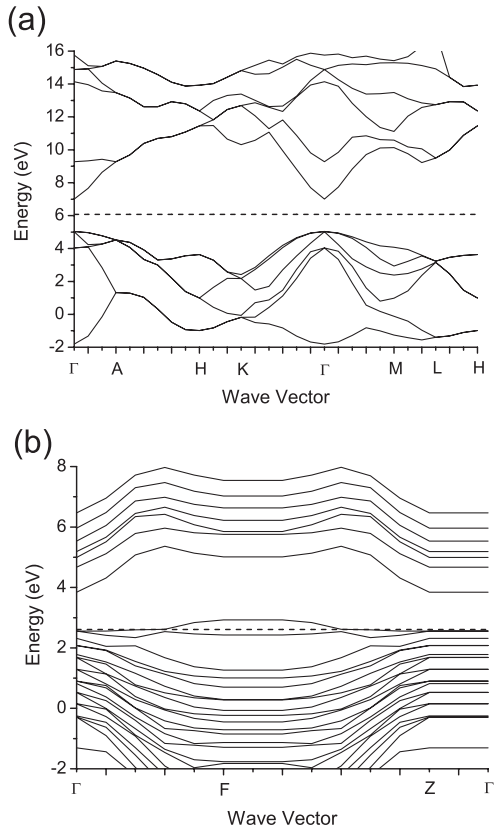

FIG. 1. Calculated band structure of GaN showing Fermi level (dashed line) (a) bulk wurtzite. (b) 16-layer GaN $(0001)/(000\bar{1})$ metallized film.

while the Be have charges of $+0.90e$ in the $(000\bar{1})$ surface bilayer and $+0.70e$ at the (0001) surface, a variation of $0.20e$, 3 times the range on the anion. Thus charge transfer from the $(000\bar{1})$ anion surface to the (0001) cation surface effectively occurs from the *cations* in the $(000\bar{1})$ surface bilayer to the *cations* in the (0001) surface. The charge on the anions is largely unaffected by the charge transfer.

Our calculations on the nonpolar $(10\bar{1}0)$ surface are in broad agreement with previous simulations for ZnO [16], AlN [17], and GaN [18]. Significant relaxations in the atomic separations ($>1\%$) are limited to the three uppermost layers at each surface. For our present purposes, the key feature is that the geometry of the surface atoms changes from sp^3 tetrahedral toward sp^2 trigonal planar coordination as the surface-layer cations contract inwards toward the slab and the anions and cations in the second layer move towards the surface. This reduces the length of the surface bonds and increases the surface bond angles from $\sim 109°$ to an average for all the compounds studied of $\sim 118°$.

For the $(0001)/(000\bar{1})$ films the bonds within each bilayer contract by $\sim 1\%$, while the bonds between the bilayers expand by $\sim 2\%$. The anion-cation-anion bond angle within each bilayer also increases by $\sim 1°$. The magnitudes of these relaxations vary with depth and for BeO, SiC, ZnO, and ZnS increase closer to the surfaces but are larger at the anion surface than the cation surface. For the nitride compounds (AlN and GaN) the separation between the bilayers increases closer to the surface but the separation within the bilayers reduces closer to the N-terminated surface. So, for example, at the $(000\bar{1})$ surface of ZnO, the separation between the outermost O and the Zn is 2.4% smaller than in the bulk and the separation between the second and third layers 7% larger. The surface bond angle (O-Zn-O) is $\sim 5.6°$ larger. As for the nonpolar surfaces, these results significantly alter the surface atom geometry away from sp^3 tetrahedral towards an sp^2 trigonal planar geometry as the bond lengths reduce and the angles increase.

For the ultrathin $(0001)/(000\bar{1})$ films there is a striking difference in the structural relaxations. When the films comprise less than a given number of layers (e.g., 18 for ZnO, see Table II) they optimize to a flat graphitic structure thus removing the destabilizing dipole. This graphitic structure arises from the atoms within each bilayer converging to just one layer, e.g., a 6-layer $(0001)/(000\bar{1})$ film will become a 3-layer graphitic film [19] with an ABAB... stacking sequence (Fig. 2). The interatomic distances within the new layers are smaller ($\sim 3\%$) than in the $(0001)/(000\bar{1})$ film but the separation between the layers is larger ($\sim 20\%$). The bond angles within a layer are hexagonal, $\sim 120°$ and we observe essentially no variation of the geometry with film thickness. The graphitic films are insulating and persist up to a set number of layers; for thicker films relaxation yields the $(0001)/(000\bar{1})$ metallized solution described above. We have only been able to find one previous report of flat films in the context of a

TABLE I. Mean Mulliken charges for the $(0001)/(000\bar{1})$ films. Also shown are the charges of the anions and cations in the surface bilayers (i.e., the surface layer and the layer adjacent to it).

	Slab Interior (e)		$(000\bar{1})$ Surface Bilayer (e)		(0001) Surface Bilayer (e)	
Film	Anion	Cation	Anion	Cation	Anion	Cation
AlN	−1.43	+1.43	−1.34	+1.59	−1.43	+1.19
BeO	−0.80	+0.80	−0.77	+0.90	−0.83	+0.70
GaN	−1.06	+1.06	−0.99	+1.19	−1.06	+0.87
SiC	−1.34	+1.34	−1.22	+1.44	−1.36	+1.07
ZnO	−0.86	+0.86	−0.86	+0.96	−0.87	+0.82
ZnS	−0.51	+0.51	−0.47	+0.55	−0.53	+0.48

TABLE II. Number of layers up to which the graphiticlike structure has a lower cleavage energy than the $(10\bar{1}0)$ and $(0001)/(000\bar{1})$ surfaces and the corresponding cleavage energies.

Film	graphitic → $(10\bar{1}0)$ number of layers	graphitic → $(10\bar{1}0)$ cleavage energy ($J\,m^{-2}$)	graphitic graphitic → $(0001)/(000\bar{1})$ number of layers	graphitic graphitic → $(0001)/(000\bar{1})$ cleavage energy ($J\,m^{-2}$)
AlN	12	3.9	24	6.5
BeO	8	2.3	30	8.6
GaN	6	2.9	12	5.5
SiC	4	3.5	8	7.7
ZnO	10	2.0	18	3.5
ZnS	4	1.4	10	5.2

wurtzite material in a theoretical study of 4-layer (0001) GaN grown on $(000\bar{1})$ SiC [20]; our calculations relate to isolated films rather than growth on a chemically different substrate. In both the metallized $(0001)/(000\bar{1})$ films and the nonpolar $(10\bar{1}0)$ film the under-coordinated surface atoms relax towards the trigonal geometry present in the graphitic solution.

Cleavage energies were calculated for each of the films by subtracting the bulk energy from the energy of the film and dividing by the area of the two surfaces created after optimization (i.e., the relaxed surfaces) [21]. Note that no unique surface energy can be determined for the (0001) and the $(000\bar{1})$ surfaces since both surfaces are present in the slab, and the cleavage energy value plotted for the nonpolar surfaces is simply twice the surface energy. The variation of the cleavage energies with the thickness of the film is plotted for the different surfaces in Fig. 3 for GaN. All the films demonstrate the same trends as those shown for GaN, the only differences being the magnitude of the cleavage energies as shown in Table II.

As expected, the nonpolar $(10\bar{1}0)$ film has a lower cleavage energy than the polar $(0001)/(000\bar{1})$ film for all thicknesses. The cleavage energy of the graphitic film rises almost linearly with the number of layers and is less than the cleavage energies of the nonpolar $(10\bar{1}0)$ film up to 4 (ZnS) and 12 (AlN) layers. This suggests that the graphitic film forms during the initial deposition of these materials which could be responsible for the formation of the polar $(0001)/(000\bar{1})$ morphology that is observed experimen-

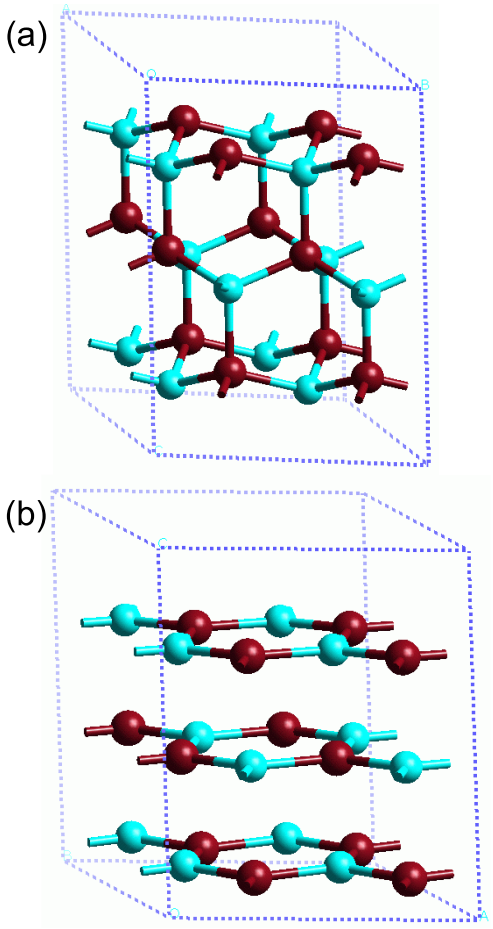

FIG. 2 (color online). Structure of 6-layer ZnO film: (a) wurtzite structure, (b) graphitic structure, where the film has optimized to a 3-layer film.

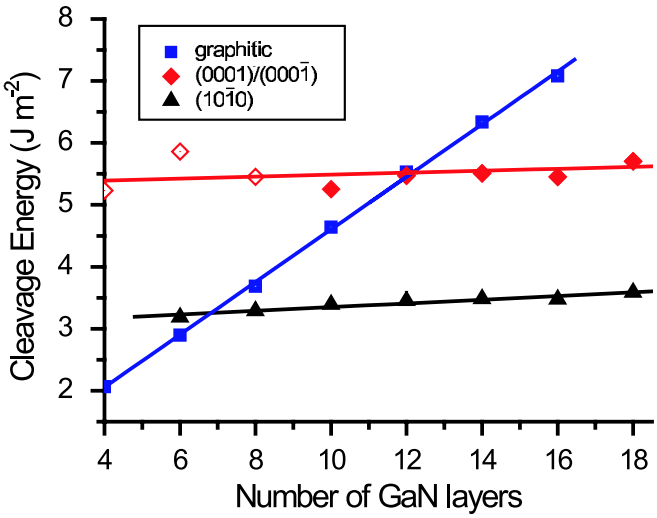

FIG. 3 (color online). Cleavage energies as a function of film thickness for GaN. For the graphitic surface the number of layers plotted is that *before* optimization. The $(0001)/(000\bar{1})$ films are unstable with respect to the graphitic structure for a small number of layers. These particular values are obtained by relaxation with a set of constraints that prevent the film optimizing to the graphitic structure and are plotted as open diamonds.

tally. Initial growth results in the graphitic film and conversion to the nonpolar, lower energy, $(10\bar{1}0)$ film is then prevented by an energy barrier arising from the substantial structural differences between the two structures (at least 0.3 eV for ZnO [15]). As the layer thickness increases, the graphitic film becomes unstable with respect to the polar $(0001)/(000\bar{1})$ film. Conversion to this film is an unactivated process and occurs in preference to the high energy conversion to the nonpolar film.

Comparing the stability of the graphitic film with respect to the $(0001)/(000\bar{1})$ film we see the graphitic structure persists up to the largest number of layers in the BeO film (30 layers). This material also demonstrates the largest relaxation of the surface atoms in the $(10\bar{1}0)$ and $(0001)/(000\bar{1})$ films toward the trigonal sp^2 geometry. Conversely, the graphitic structure persists up to the fewest number of layers in the SiC and ZnS materials, which demonstrate the smallest relaxations for the $(10\bar{1}0)$ and $(0001)/(000\bar{1})$ films towards the sp^2 geometry. This suggests a relationship between the chemical components of the films and the preference for the graphitic structure. The atoms in the graphitic structure adopt a planar threefold coordination, while those in the wurtzite structure have a tetrahedral geometry. C, N, and O readily form sp^2- hybridized multiple bonds in a wide variety of molecules [22], while 2nd row elements such as S adopt a threefold planar coordination much more reluctantly due to the relative weakness of their multiple bonds. Thus, the graphitic structure should persist in thicker films containing 1st row elements compared to those with 2nd row elements. In addition, the graphitic structure is insulating in contrast to the metallized surfaces of the $(0001)/(000\bar{1})$ films. In order for the insulating graphitic system to metallize and convert to the $(0001)/(000\bar{1})$ film there must be an associated charge transfer. We might expect that this would be related to the band gap and electronegativity of the elements: the larger the band gap and the more electronegative the anions the more difficult the metallization. This is consistent with the calculated band gaps of the graphitic film. For example, the graphitic structure persists up to 24 layers for AlN compared to only 12 for GaN and the band gap for the AlN graphitic film is 3.19 eV compared to 2.11 eV for GaN. The coordination preferences of the atoms and electronic structure clearly influences the stability of the graphitic structure with respect to the metallized $(0001)/(000\bar{1})$ film.

In summary, we have used *ab inito* calculations to model the polar $(0001)/(000\bar{1})$ and nonpolar $(10\bar{1}0)$ surfaces of a range of wurtzite materials. We demonstrate that the charge transfer model proposed by Wander *et al.* [9] and Carlsson [10] for the stabilization of the polar (0001) and $(000\bar{1})$ surfaces can operate for AlN, BeO, GaN, SiC, and ZnS in addition to ZnO. For both the polar and nonpolar surfaces we have recorded surface relaxations which change the surface atom geometry from sp^3 to sp^2 geometries. For the $(0001)/(000\bar{1})$ ultrathin films of AlN, BeO, GaN, SiC, and ZnS we have also investigated a new graphitic film structure which is lowest in energy for all these systems. The graphitic film may explain the growth of the polar $(0001)/(000\bar{1})$ film in preference to the nonpolar $(10\bar{1}0)$ film. The stability of the graphitic structure relative to a film terminating with the $(0001)/(000\bar{1})$ surfaces varies from film to film and we have discussed the factors controlling the relative stability of this surface.

This work is supported by EPSRC Grants No. GR/85952 and No. GR/85969.

[1] P. X. Gao, Y. Ding, W. Mai, W. L. Hughes, C. Lao, and Z. L. Wang, Science **309**, 1700 (2005).
[2] J. Goldberger, R. He, Y. Zhang, S. Lee, H. Yan, H.-J. Choi, and P. Yang, Nature (London) **422**, 599 (2003).
[3] M. H. Huang, S. Mao, H. Feick, H. Q. Yan, Y. Y. Wu, H. Kind, E. Weber, R. Russo, and P. D. Yang, Science **292**, 1897 (2001).
[4] P. W. Tasker, J. Phys. C **12**, 4977 (1979).
[5] C. Noguera, J. Phys. Condens. Matter **12**, R367 (2000).
[6] J. Fritsch, O. F. Sankey, K. E. Schmidt, and J. B. Page, Phys. Rev. B **57**, 15 360 (1998).
[7] J. E. Northrup, R. D. Felice, and J. Neugbauer, Phys. Rev. B **55**, 13 878 (1997).
[8] O. Dulub, L. A. Boatner, and U. Diebold, Surf. Sci. **519**, 201 (2002).
[9] A. Wander, F. Schedin, P. Steadman, A. Norris, R. McGrath, T. S. Turner, G. Thornton, and N. M. Harrison, Phys. Rev. Lett. **86**, 3811 (2001).
[10] J. M. Carlsson, Comput. Mater. Sci. **22**, 24 (2001).
[11] M. C. Payne, M. P. Teter, D. C. Allan, T. A. Arias, and J. D. Joannopoulos, Computer code CASTEP 4.2, Academic version, Licensed under the UKCP-MSI Agreement, 1999 [Rev. Mod. Phys. **64**, 1045 (1992)].
[12] J. P. Perdew and Y. Wang, Phys. Rev. B **45**, 13 244 (1992).
[13] D. Vanderbilt, Phys. Rev. B **41**, 7892 (1990).
[14] H. J. Monkhorst and J. D. Pack, Phys. Rev. B **13**, 5188 (1976).
[15] F. Claeyssens, C. L. Freeman, N. L. Allan, Y. Sun, M. N. R. Ashfold, and J. H. Harding, J. Mater. Chem. **15**, 139 (2005).
[16] N. Jedrecy, S. Gallini, M. Sauvage-Simkin, and R. Pinchaux, Surf. Sci. **460**, 136 (2000).
[17] A. Filippetti, V. Fiorentini, G. Cappellini, and A. Bosin, Phys. Rev. B **59**, 8026 (1999).
[18] J. Northrup and J. Neugebauer, Phys. Rev. B **53**, R10 477 (1996).
[19] The graphitic films are labeled by their starting number of layers for comparison with the other films, e.g., a 6-layer film that has optimized to a 3-layer film is still referred to as a 6-layer film.
[20] R. B. Capaz, H. Lim, and J. D. Joannopoulos, Phys. Rev. B **51**, 17 755 (1995).
[21] The bulk energy is taken as the bulk energy of the wurtzite phase in all cases including the graphitic film, so that the energies of the different structures in Fig. 3 can be compared directly from the cleavage energies plotted.
[22] N. N. Greenwood and A. Earnshaw, *Chemistry of the Elements* (Reed Educational and Professional Publishing, Ltd., Oxford, 1997), 2nd ed.